Studiegroep Wiskunde met de Industrie 2003

pp. 21 – 44

CHAPTER 2

Japanese Oysters in Dutch Waters

Jan Bouwe van den Berg, Gregory Kozyreff, Hai-Xiang Lin, John McDarby, Mark A. Peletier, Robert Planqué, Phillip L. Wilson

Other participants:

Dragan Bezanovic, Luca Ferracina, Joris Geurts van Kessel[1], Belinda Kater[1], Kamyar Malakpoor, Harmen van der Ploeg, José A. Rodríguez, Bart van de Rotten, Karin Troost[1], Nienke Valkhoff, and J.F. Williams

Abstract. We study a number of aspects of the colonisation of the Eastern Scheldt by the Japanese Oyster. We formulate and analyse some simple models of the spatial spreading, and determine a rough dependence of the spreading behaviour on parameters. We examine the suggestion of reducing salinity by opening freshwater dams, with the aim of reducing oyster fertility, and make predictions of the effect of such measures. Finally, we present an outline of a large-scale simulation taking into account detailed data on the geometry and sea floor properties of the Eastern Scheldt.

Keywords: Japanese Oyster, *Crassostrea gigas*, population dynamics

1. Introduction

In 1964 the Japanese Oyster (*Crassostrea gigas*) was introduced into the Eastern Scheldt. It was believed that this species could not breed in the colder Dutch climate; each generation would have to be set out by hand. Therefore this introduction was expected to have limited impact on the local ecosystem. Additionally, at that time the plan was to close off (part of) the Eastern Scheldt, so that even if spawning occurred, the problem would remain local.

Unfortunately the brief hot spells of some Dutch summers allowed the Japanese Oysters to spawn. With a maximal life span of thirty years the population proved able to spawn in the rare hot years and simply survived in other years. As a result, the Japanese Oyster is now a dominant species in the Eastern Scheldt; the indigenous flat oyster (*Ostrea edulis*) has disappeared almost completely (mainly due to disease and the very cold winter of 1963), the cockles are declining in number, and mussels have been confronted by a the appearance of a strong competitor for food. In addition, the Japanese Oyster has spread beyond the Eastern Scheldt and

[1]We would like to direct special thanks to the proposers of the problem for the information and data provided, the corrections suggested and the hospitality in Yerseke.

FIGURE 1. A bank of Japanese Oysters

settled in parts of the Western Scheldt and the Wadden Sea. At present, the main negative impact is that the Japanese Oysters compete with cockles for space and food. In turn, the decline in cockles causes problems for the birds that feed on them.

At the Study Group two Dutch institutes, the Nederlands Instituut voor Visserijonderzoek (The Netherlands institute for fisheries research[2]) and Rijksinstituut voor Kust en Zee (RIKZ, The Netherlands institute for coastal and marine management) presented the issue of the spreading of the Japanese Oysters. The following questions were formulated:

How do oysters spread?
Can development in the past be reconstructed?
Can a prediction be made for the future?
Can the spreading of the oysters be stopped? How?

2. Overview

In this report we address these questions from a number of different viewpoints. Let us give an overview of the different models and their outcomes up front.

- In Section 3 we present a first study of the spreading of oysters. We assume a favourable (i.e. hard) substrate and model the spread of oysters from year to

[2]Formerly known as RIVO, presently part of Animal Sciences Group.

FIGURE 2. Map of the Eastern Scheldt

year. We indicate how to extend this model to perform simulations to reconstruct the spreading of oysters from 1964 onwards.

- In Section 4 we simplify the model of Section 3 by passing to continuous time, and compare spreading velocities between soft and hard substrates. We find a significant difference in spreading velocity, and argue that the ratio of the two velocities is relatively independent of the important parameters, which are difficult to estimate.
- In Section 5 we study a proposed remedy of re-opening the dams that currently prevent river water from entering the Eastern Scheldt. The reduction in salinity that results from the influx of fresh water may reduce the growth rate of the oysters. In extension of a recent simulation at RIKZ we consider a scenario of partial, seasonal re-opening of the dams, and find that the effect on salinity is similar (to a permanent reopening scenario), but with some advantages. The main conclusion, however, is that the proposed regulation of salinity is not sufficient to significantly control the growth of oysters in the Eastern Scheldt.
- In Section 6, finally, we present an outline of a large-scale simulation that takes into account the detailed geometry and geology (e.g. substrate hardness) of the Eastern Scheldt. This simulation might be implemented as an extension of a code that is currently in use at Rijkswaterstaat.

3. Diffusion of larvae

At the end of July of a hot year, the rising of the sea temperature over a certain threshold triggers a massive production of oyster larvae. During their 15–30 day life span, these larvae are passively transported by the flow in random directions until they settle. This transport is probably the main mechanism by which *Crassostrea gigas* invaded the whole Eastern Scheldt. In this section, we will analyse this mechanism, in conjunction with a simple model of the interaction between the oyster and larvae populations. We will restrict our attention to the eastern part of the Eastern Scheldt, where the *Crassostrea gigas* was introduced, in 1964. Indeed, this region is characterised by relatively shallow water and weak currents, which hampers the geographic progression of oysters. Because of this, it took years before the oyster population reached the central part of the Eastern Scheldt. Afterwards, larvae became subjected to much stronger currents and were therefore prone to colonise the rest of the Eastern Scheldt in a relatively short period. At least, this is one of the possible scenarios. Slow adaptation of the Japanese Oysters to the local environment may also have contributed to the time delay before the central part was reached. Probably a combination of factors, partly due to the construction of the Delta works, has caused the explosion of Japanese Oysters in the Eastern Scheldt.

The simplest description of the geographical spreading of oysters should comprise two independent variables: one for the larvae population and one for the oysters. Hence we introduce:

- $\mathcal{O}_n(x)$: the density of oysters, expressed in m^{-2}, in year n. $\mathcal{O}_n$ depends on the position x (which is one-dimensional, for simplicity);
- $\mathcal{L}_n(x,t)$: the density, also expressed in m^{-2}, of larvae in the summer of year n. $\mathcal{L}_n$ depends on position x and time t.

During their short life, we model the transport of larvae by a reaction-diffusion equation of the form:

$$\frac{\partial \mathcal{L}_n}{\partial t} = D_T \frac{\partial^2 \mathcal{L}_n}{\partial x^2} + Q\left(\mathcal{L}_n, \mathcal{O}_n\right). \tag{1}$$

In this equation, the first two terms describe the diffusive transport averaged over an entire tidal cycle. The last term Q accounts both for the production and the disappearance of larvae, either by death or by settlement on the ground. A crucial parameter is the diffusion coefficient D_T and we will estimate it below. As for the oysters, their density varies from year to year according to:

$$\mathcal{O}_{n+1} = \mathcal{O}_n + G\left(\mathcal{L}_n, \mathcal{O}_n\right), \tag{2}$$

where G is the number of newly born oysters minus the deceased ones per unit area. For the moment, we do not specify the functionals Q and G. Several choices of Q and G will be presented in this report and many variations are possible. The choice between these requires a delicate balancing of the questions that are to be addressed, on one hand, with the available data on the other. More complex models, often used for the purpose of tracking growth in cultivated oysters, sort the individuals by sizes and introduce as many oyster variables as there are size-classes [**3**]. In

this work, motivated by the relative lack of data[3], we discard such aspects of the dynamics and, with the exception of the final Section, focus on models of minimal complexity.

In the following sections we first model the spreading of oysterlarvae to determine D_T. (in §3.1). Then we discuss the factors that influence the growth, survival and reproduction of oysters and larvae, and we present the outcome of the model (in §3.2). Finally, in §3.3, a continuous time limit is derived, which serves as a connection to the continuous time model discussed in Section 4.

3.1. Diffusion-convection over a single tidal cycle. On the time scale of a tidal cycle the larvae are subject to a tidal flow. With u the water velocity generated by the tides, the transport equation for the larvae becomes (setting $Q = 0$ for the present discussion)

$$\frac{\partial \mathcal{L}}{\partial t} + u\frac{\partial \mathcal{L}}{\partial x} = D\left(\frac{\partial^2 \mathcal{L}}{\partial x^2} + \frac{\partial^2 \mathcal{L}}{\partial z^2}\right), \tag{3}$$

where D is the coefficient of diffusion in the absence of tide and where $\mathcal{L}$ is assumed to depend on the vertical coordinate z too.

As was first recognised by Taylor [**15**], a nonuniform vertical distribution of u accelerates the dispersion of particles. This can be understood by noting that at a depth z where u is maximal, particles (e.g. larvae) are likely to travel over much longer distances than those at depths where u is small.

If $u = u(z)$, one can show that equation (3) can be approximated in the long time limit by the following, simpler equation:

$$\frac{\partial \mathcal{L}}{\partial t} + U_0\frac{\partial \mathcal{L}}{\partial x} = (D + D_T)\frac{\partial^2 \mathcal{L}}{\partial x^2}, \tag{4}$$

where U_0 is the average velocity of the flow over the z-direction. While equation (4) applies to the rising tide, the falling tide is described by

$$\frac{\partial \mathcal{L}}{\partial t} - U_0\frac{\partial \mathcal{L}}{\partial x} = (D + D_T)\frac{\partial^2 \mathcal{L}}{\partial x^2}. \tag{5}$$

Hence, averaging over many tides, one obtains

$$\frac{\partial \mathcal{L}}{\partial t} = (D + D_T)\frac{\partial^2 \mathcal{L}}{\partial x^2}. \tag{6}$$

Since we are primarily interested in the diffusion of larvae in the horizontal directions, and owing to its relative simplicity, equation (6) represents progress from equation (3).

With the sea level and sea bed respectively denoted by h and z_0, the new diffusion coefficient is given by [**11**]

$$D_T = \frac{U_0}{D(h - z_0)}\int_{z_0}^{h}\left[\int_{z_0}^{z}\left(1 - \frac{u(z')}{U_0}\right)dz'\right]^2 dz. \tag{7}$$

Our first task will therefore be to assess the velocity profile u resulting from the tidal flow. Actually, u depends on x as well as z. Hence, $D_T = D_T(x)$ and equation (4) has to be slightly modified, as shown in the appendix.

[3]Data are hard to obtain since experiments are difficult and time consuming.

3.1.1. *Tidal flow.* For a shallow part of the sea the determination of u is relatively simple. Let the elevation of the sea bed be denoted by $z_0(x)$. As a result of the tides, the sea level is a function of time and given by $z = h(t)$. From the "shallowness" hypothesis, and assuming low velocities, the Navier-Stokes equations for the flow reduce to:

$$0 = -\frac{dp}{dx} + \mu \frac{\partial^2 u}{\partial z^2}. \tag{8}$$

In this equation, p is the pressure and μ is the viscosity of water. This equation must be supplemented by two boundary conditions. One is that the velocity vanishes on the sea bed, $u(z_0) = 0$. The other is that the sea surface is free of any applied stress, which translates into $\frac{\partial u}{\partial z}(h) = 0$. This allows to write the solution of (8) as:

$$\begin{aligned} u(x,z) &= \frac{1}{2\mu}\frac{dp}{dx}(z-z_0)(z-2h+z_0), \\ &= C(z-z_0)(z-2h+z_0). \end{aligned} \tag{9}$$

In this expression the constant C is determined from the conservation of mass. Considering a slice dx of fluid, the rise or fall of its level, $\frac{dh}{dt}$, is only due to incoming and outcoming flux of water on either sides of the slice. This leads to the equation

$$\frac{dh}{dt} + \frac{\partial}{\partial x}\int_{z_0}^{h} u(x,z)\,dz = 0. \tag{10}$$

Substituting (9) into (10), we find:

$$u(x,z) = \frac{3}{2}U_0 \frac{(z-z_0)(2h-z-z_0)}{(h-z_0)^2}, \tag{11}$$

where U_0 is the average velocity, given by

$$U_0 = \frac{dh/dt}{dz_0/dx}. \tag{12}$$

3.1.2. *Estimation of D_T.* The value of D is estimated to be $10^{-4}\,\mathrm{m^2 s^{-1}}$ for stratified flow and $10^{-3}\,\mathrm{m^2 s^{-1}}$ for well mixed flows [**17**]. These values are obtained by measuring the diffusion in the vertical direction, which is not affected by the tidal flow. During the rising tide, the sea level rises by 3 meters in 6 hours, and we assume the slope of the sea bed to be 1%. Hence, U_0 is estimated to be

$$U_0 \approx \frac{3\,\mathrm{m}/(6\cdot 3600\,\mathrm{s})}{0.01} \approx 0.02\,\mathrm{m s^{-1}}.$$

Then, substituting expression (11) into (7), we obtain:

$$D_T = \frac{2U_0(h-z_0)^2}{105D}. \tag{13}$$

Hence, with a sea depth of 3-4 m, a vertical diffusion D of $10^{-3}\,\mathrm{m^2 s^{-1}}$ and our estimate of U_0, we get

$$D_T \approx 0.1\,\mathrm{m^2 s^{-1}},$$

which is considerably larger than D.

As we already noted, D_T is a function of x. It is therefore tempting to simply rewrite the diffusion term in the right hand side of (6) as $\frac{\partial}{\partial x}D_T(x)\frac{\partial}{\partial x}\mathcal{L}$. However,

one must bear in mind that the effective parameter $D_T(x)$ encompasses more than just Fick's law of transport. The actual reduced diffusion equation turns out to be (see the appendix)

$$\frac{\partial \mathcal{L}}{\partial t} = D_T \left[\left(1 + \frac{D}{D_T} \right) \frac{\partial^2 \mathcal{L}}{\partial x^2} - \frac{12\,(dz_0/dx)}{(h - z_0)} \frac{\partial \mathcal{L}}{\partial x} \right]. \tag{14}$$

For simplicity, in what follows, we will neglect spatial variations of D_T.

3.2. Completion of the model and outcome. In order to be able to forecast the expansion of the oysters, one needs to choose sensible and simple forms for Q and G.

Female and male oysters are able to detect the presence of eggs and sperm in the water [**12**]. In order to maximise fecundation, they all release their gametes at the same time. Accordingly, the production of larvae is modelled by the initial condition

$$\mathcal{L}_n(x, 0) = F \mathcal{O}_n, \tag{15}$$

where F is the fecundity of an oyster and is the combination of several factors, such as the size of the oyster, the salinity of water and the likelihood of an egg to be fertilised. An expression derived from observation is [**9**]

$$F = F_l F_s F_f$$

with

- $F_l = 0.4\, l^{2.8}$: size factor, where l is the size of the oyster in cm.
- $F_s = \frac{s-8}{5.5}$: salinity factor, where s is the salinity of water, expressed in grams of chloride per liter,
- $F_f = 0.005\, \mathcal{O}_n^{0.72}$: fertilisation efficiency.

Besides, since the larvae only have an approximate 15–30 day life span, one includes a death rate in the larvae equation:

$$\begin{aligned} \frac{\partial \mathcal{L}_n}{\partial t} &= D_T \frac{\partial^2 \mathcal{L}_n}{\partial x^2} - \frac{\mathcal{L}_n}{t^*}, \\ t^* &= 30 \text{ days}. \end{aligned} \tag{16}$$

Of the larvae that are transported according to this equation, only a tiny fraction λ will actually be able to settle. The magnitude of this fraction depends on a number of factors, among which the hardness of the substrate and the presence of other oysters. For the length of this section we will assume that the substrate is hard, providing a good environment for settling larvae. In Section 4 we study the effect of substrate hardness in detail.

Presence of other oysters on the substrate will result in competition for nutrient and predation of larvae from the mature oysters. This overcrowding factor is supposed to be only effective when the oyster density passes a certain threshold $\mathcal{O}_{sat}$. Finally, approximately one tenth of the oyster population dies each year [**3**]. These considerations lead to the following equation for the oyster population

$$\mathcal{O}_{n+1}(x) = \mathcal{O}_n(x) + \frac{\lambda \mathcal{L}_n(x, t^*)}{1 + \mathcal{O}_n(x)/\mathcal{O}_{sat}} - \frac{\mathcal{O}_n(x)}{10} \tag{17}$$

From the observation of actual oyster banks, $\mathcal{O}_{sat}$ ranges between $30\,\mathrm{m}^{-2}$ and $100\,\mathrm{m}^{-2}$.

Prior to the integration of equations (15)-(17), it is useful to introduce dimensionless variables as

$$T = \tfrac{t}{t^*}, \quad X = \tfrac{x}{(D_T t^*)^{1/2}} \approx \tfrac{x}{400\,\mathrm{m}},$$
$$u_n = \tfrac{\lambda \mathcal{L}_n}{\mathcal{O}_{sat}}, \quad v_n = \tfrac{\mathcal{O}_n}{\mathcal{O}_{sat}}.$$

The system of equations to solve for each year thus becomes

$$\frac{\partial u_n}{\partial T} = \frac{\partial^2 u_n}{\partial X^2} - u_n, \tag{18}$$

$$u_n(X,0) = \Lambda v_n(X), \tag{19}$$

$$v_n = 0.9 v_{n-1} + \frac{u_{n-1}(X,1)}{1+v_{n-1}}. \tag{20}$$

In these equations, the only free parameter that remains is

$$\Lambda = \lambda F.$$

It represents the number of newly born oysters per oyster per year in the absence of overcrowding effect. Each year, n, the diffusion equation (18) is integrated with initial condition (19) and the oyster population is updated according to (20).

From 1964 onwards, oysters were introduced and cultivated on 100 m wide squares approximately 8 km away from the central region. In the new space scale, $100\,\mathrm{m} \to 0.25$ and $8\,\mathrm{km} \to 20$. We assume now that there has been (a small amount of) spawning every year since the introduction in 1964. The first settling of oyster larvae, called spat at this stage, on dike foots and jetties was recorded in 1976. Hence, we need to integrate the system above for 12 years, $n = 1, \ldots, 12$, and check whether a significant number of oyster/larvae could reach the central region. Initially, the oyster distribution is given by

$$v_0(X) = \begin{cases} 1, & 0 < X < 0.25, \\ 0, & 0.25 < X. \end{cases}$$

It is a simple task to integrate numerically the system (18)-(19) with the initial condition above. The result is shown in Figure 3 and suggests that the development in the past can indeed be constructed with this simple model provided that $\Lambda \geq$ 8-10.

3.3. Continuous time dependence for oysters. To close this section, let us remark that the system (18)-(19) can be made amenable to further analytical development by turning the difference equation (20) into a differential one. Indeed, assuming that the variation of oyster population density is small from year to year, one can write

$$v(n+1) \approx v(n) + \frac{\partial v}{\partial n},$$

where n is now considered as a continuous variable that measures time in units of years. One thus has: $n = \frac{t}{\mathrm{year}} = \frac{t}{\mathrm{month}} \frac{\mathrm{month}}{\mathrm{year}} = \varepsilon T$, so that, generally, the

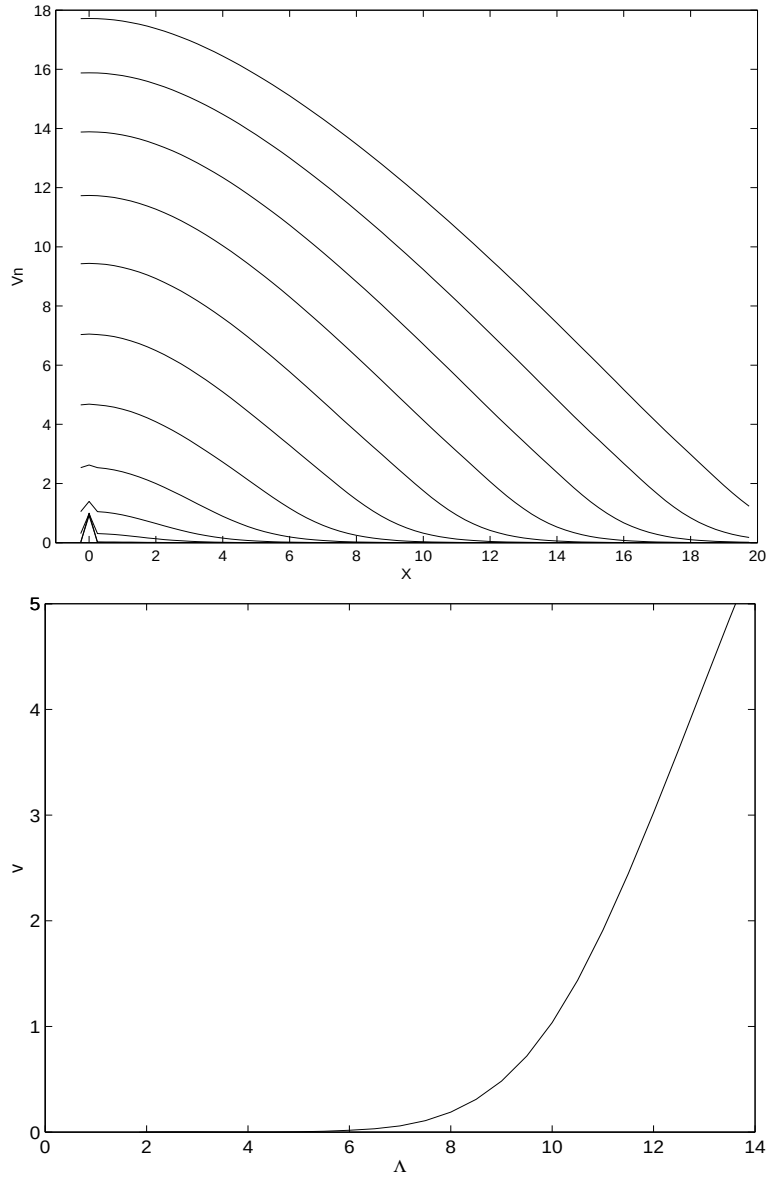

FIGURE 3. Yearly evolution of the oyster distribution v_n with $\Lambda = 10$ (top) and oyster density v_{12} at the border of the Eastern region for various values of Λ after 12 years (bottom).

larvae/oyster model can be cast in the following form

$$\varepsilon \frac{\partial u}{\partial n} = \frac{\partial^2 u}{\partial X^2} + Q, \tag{21}$$

$$\frac{\partial v}{\partial n} = G. \tag{22}$$

3.4. Discussion. In this section we have sketched a way to model the oyster expansion in the Eastern Scheldt. The simplest choice of the generation rates Q and G of larvae and oysters, respectively, already proves quite informative. After rescaling variables, only one free parameter remains: Λ, the number of descendants per oyster per year in the absence of any overcrowding effects. It was found that Λ needs to be in the order of 10 in order to reconstruct a specific aspect of the history of oyster proliferation, the time lapse between the introduction in 1964 and the first large-scale sightings in 1976. Although this value may appear large, one must bear in mind that it does not account for overcrowding effects. Moreover, the more accurate diffusion model (19) would probably require smaller values of Λ, owing to the dependence of D_T on the sea depth.

Although the proliferation of oysters was only observed in 1976, the present analysis suggests that it had actually been taking place right from the beginning of their implantation in 1964. Because it was under water and at some distance from the shores and coasts, it is possible that the process went unnoticed before 1976.

Let us finally note the large values attained by the oyster density in figure 3. This results from the relatively long life span of oysters. However, overcrowding should be taken into account in the death rate of oysters. It is indeed observed that oysters grow on top of each other, so that only the top layer is alive. This point is (at least partially) addressed in the next sections.

4. The effect of substrate hardness on the spreading of an oyster bank

In this section we study the spreading of an oyster bank where we concentrate on the phenomenon that oysters prefer to settle on a hard substrate rather than a sandy one.

4.1. The Fisher-Kolmogorov equation. The classical model [**10**] for spatial spreading of any biological species is the Fisher-Kolmogorov (FK) equation

$$\frac{\partial u}{\partial t} = D\Delta u + f(u), \tag{23}$$

where Δ is the Laplacian (in the spatial coordinates), D the diffusion constant and f is a nonlinear function, typically

$$f(u) = u(1-u) \tag{24}$$

or

$$f(u) = u(u-a)(1-u) \quad \text{with } 0 \leq a \leq 1. \tag{25}$$

The Fisher-Kolmogorov equation has been analysed in excruciating detail. We will only recall a few results here to serve as a guide for a more specialised model presented in §4.2.

In the present context u can be interpreted as the biomass of the oysters (or their number) per unit area. The crucial difference between the nonlinearities (24) and (25) is that for the former the trivial equilibrium $u = 0$ is unstable while for the latter it is stable (at least in the absence of diffusion). The equilibrium $u = 1$ is stable in both cases. We will refer to (24) as the monostable case and to (25) as the bistable case. One interpretation is that the monostable case corresponds

to oyster growth on a hard substrate (rocks or concrete), whereas the bistable case corresponds to oyster growth on a soft substrate (a sand bank). Without going into a biological interpretation we now state some mathematical results. In §4.2 we discuss the choice of nonlinearities in more detail.

The dynamics of solutions of (23) are dominated by travelling wave solutions, i.e., solutions of the form $u = U(x - ct)$, where c is the speed of the wave, and x is the direction of propagation. The waves of interest are those connecting the solutions $u = 0$ (no oysters) and $u = 1$ (thriving oyster population).

In the monostable case there exist travelling waves with arbitrarily large speed, hence a priori the oysters could spread at arbitrarily large rates. However, "most" solutions, in particular those starting from compactly supported initial data (corresponding to a well-defined bank of oysters), select the velocity $c_{\text{mono}} = 2\sqrt{D}$, which is also the minimal speed among the everywhere positive travelling waves.

In the bistable case there is a unique travelling wave; it has velocity $c_{\text{bi}} = (1 - 2a)\sqrt{\frac{D}{2}}$. Hence for $a < \frac{1}{2}$ the oysters spread, i.e. $u = 1$ "invades" $u = 0$. Clearly $c_{\text{mono}} < c_{\text{bi}}$ for any $a \in [0, 1/2)$. Although this information has limited value since we have ignored implicit scalings in the argument, the idea is that the oysters spread more rapidly on a hard than on a soft substrate. With these differences in mind we now turn to a more detailed model which incorporates both oysters and larvae.

4.2. An oyster-larvae model. We consider a model which takes into account two stadia in the life cycle of an oyster with obviously different dynamic capabilities, namely oysters which are fixed to the seabed and larvae which float around in the sea. We thus disregard (or assume insignificant) the fact that oysters may detach from the seabed and move to more favourable grounds. Of course there are many other features that we do not include in our model either.

From Section 3 we pick up the discussion at the continuous-time system of equations (21-22). We briefly return to the dimensional variables $\mathcal{O}$ and $\mathcal{L}$ for oysters and larvae. Assuming that the larvae diffuse (with diffusion constant D), die at rate E (per unit time) and that (as in Section 3) each oyster produces F larvae per unit time, we obtain the equation (analogous to equation (1), with a particular choice of Q)

$$\mathcal{L}_t = D\mathcal{L}_{xx} - E\mathcal{L} + F\mathcal{O}. \tag{26}$$

Here subscripts denote partial derivatives. For simplicity (and since we are going to look at travelling waves anyway) we take into account only one spatial dimension.[4]

The more interesting part of the model is the choice of the nonlinearity G which describes the transition of larvae to oysters. We assume that the increase in oyster population is proportional to the amount of larvae (with proportionality constant A), and that the growth saturates when the oysters reach some maximal density

[4]As explained in §3.3, this equation represents a smoothed version of the discrete-time equation of the previous section. Assuming a reference time scale of a year, the coefficients D and E in this equation are the natural coefficients associated with diffusion and death of the larvae, per year. The coefficient F, on the other hand, should be viewed as the production of larvae, per oyster, averaged over a year.

$\mathcal{O}_{sat}$ due to competition for food and/or space (which makes it harder for larvae to settle). Additionally, we include a death rate C. This leads to

$$\mathcal{O}_t = A\mathcal{L}(1 - \mathcal{O}/\mathcal{O}_{sat}) - C\mathcal{O}. \tag{27}$$

Since the oysters are immobile there is no diffusion term. Alternatively, when the sea bed is sandy, the larvae prefer to settle on existing oysters (dead or alive), which we model by

$$\mathcal{O}_t = A\mathcal{L}(\mathcal{O}/\mathcal{O}_{sat} + \delta)(1 - \mathcal{O}/\mathcal{O}_{sat}) - C\mathcal{O} \tag{28}$$

with $0 \leq \delta \ll 1$ a (dimensionless) measure for the relative preference of larvae to settle on a soft compared to a hard substrate. We note that the choice $\delta = 0$ prevents spreading of oysters to previously unoccupied territory: since equation (28) contains neither diffusion nor convection, $\mathcal{O}(x, 0) = 0$ implies $\mathcal{O}(x, t) = 0$ for all $t \geq 0$.

For (27), in combination with (26), the trivial equilibrium $(\mathcal{L}, \mathcal{O}) = (0, 0)$ is unstable provided $AFE^{-1} < C$, while for (28) it is stable provided $\delta AFE^{-1} < C$ (the inequalities have an obvious interpretation). In the following we will assume that

$$\delta < \frac{CE}{AF} < 1. \tag{29}$$

The situation is thus very similar to the comparison between the monostable and bistable cases for the scalar equation in §4.1.

In true study group spirit, some educated guesses for the parameters are

$$\begin{array}{llllll} A: & 10^{-5}\,\mathrm{y}^{-1} & \mathcal{O}_{sat}: & 10^{2}\,\mathrm{m}^{-2} & C: & 10^{-1}\,\mathrm{y}^{-1} \\ D: & 10^{-1}\,\mathrm{m}^{2}\mathrm{s}^{-1} & E: & 3\cdot 10^{1}\,\mathrm{y}^{-1} & F: & 10^{7}\,\mathrm{y}^{-1} \qquad \delta: \quad 10^{-2} \end{array} \tag{30}$$

The death rates C and E follow from the life span of the oysters and of the larvae; the maximal oyster density $\mathcal{O}_{sat}$ is estimated from existing oyster banks; the diffusion coefficient D was estimated in Section 3 (and then called $(D + D_T)$); the larvae production per oyster per year F and the ratio δ were estimated by experts from the Animal Sciences Group. The larvae-to-oyster transformation rate A (under optimal conditions) is difficult to estimate. The second inequality in (29) implies the bound $A > 3 \cdot 10^{-7}\,\mathrm{y}^{-1}$; we chose the value $10^{-5}\,\mathrm{y}^{-1}$ to accommodate this inequality.

Introduce the dimensionless variables

$$\tilde{u} = E(\mathcal{O}_{sat}F)^{-1}\mathcal{L}, \quad \tilde{v} = \mathcal{O}_{sat}^{-1}\mathcal{O}, \quad \tilde{x} = \sqrt{E/D}x, \quad \tilde{t} = Et,$$

and the dimensionless parameters

$$\alpha = AFE^{-2} \qquad \text{and} \qquad \beta = CE(AF)^{-1}.$$

(The parameter α is closely related—approximately equal—to the combined parameter $\varepsilon\Lambda$ of the previous section. It is the growth rate of the system without diffusion, without oyster morbidity, without taking crowding into account, and with $\delta = 0$). After dropping the tildes from the notation we obtain

$$\begin{cases} u_t = u_{xx} - u + v, \\ v_t = \alpha[u(v^k + k\delta)(1 - v) - \beta v]. \end{cases} \tag{31}$$

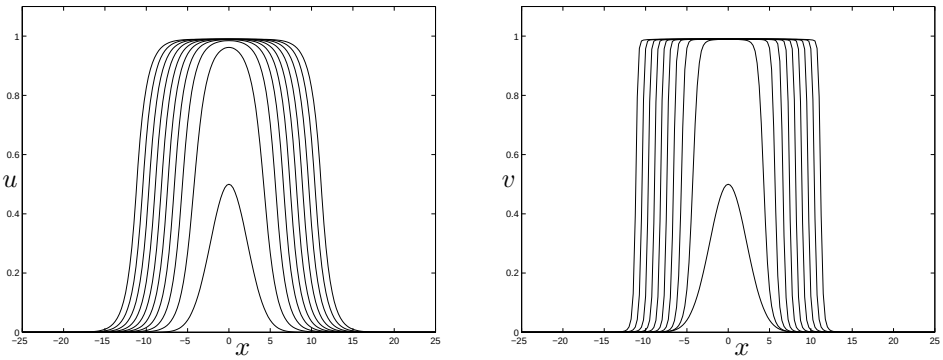

FIGURE 4. A solution of (31) with $k = 1$, $\alpha = 1$, $\beta = 10^{-2}$, $\delta = 10^{-3}$ showing the development towards travelling waves.

Here $k = 0$ or $k = 1$, corresponding to a hard and a soft substrate respectively. We recall that we assume $0 \leq k\delta < \beta < 1$ (which is satisfied if the estimated values (30) are approximately correct, namely $\beta = 3 \cdot 10^{-2} \ll 1$).

As for the FK equation in §4.1 we expect the long term dynamics to be dominated by travelling waves and this is confirmed by numerical simulations, see Figure 4.

Our discussion of (31) now follows the lines of that of the FK equation. For the hard substrate ($k = 0$) we look at the asymptotic case $\beta = 0$. The trivial state is unstable and we can expect there to be a one parameter family of travelling waves, one of which is selected by sufficiently localised initial data. The expected asymptotic velocity c_h can be calculated explicitly; here we did so by locating the value of c for which two eigenvalues coincide. Under the condition that c should be real, this value is unique. The result is depicted in Figure 5 as a function of the parameter α. In the limits of small and large α the behaviour is

$$c_h \sim \sqrt{\tfrac{27}{4}\alpha} \quad \text{as } \alpha \to 0, \qquad\qquad c_h \sim \sqrt[4]{\tfrac{27}{4}}\alpha^{1/4} \quad \text{as } \alpha \to \infty.$$

Numerical calculation show that the speed c_h thus calculated analytically is indeed the selected wave speed.

For the soft substrate ($k = 1$) the limit case $\beta \to 0$ also implies $\delta \to 0$ because of the requirement $\delta < \beta$. However, it is not clear that this limit is well-defined. Therefore, for the moment we will use the values $\beta = 3 \cdot 10^{-2}$ and $\delta = 10^{-2}$ which follow from (30). In any case it is impossible to calculate the (unique) wave speed analytically, so we have to rely on numerical computations. The asymptotic speed c_s is depicted in Figure 5, again as a function of the parameter α.

4.3. Discussion. For $\alpha = 10^{-1}$, the value corresponding to (30), we have $c_h = 0.2$ and $c_s = 0.01$. These numbers can be interpreted in two ways:

- A speed $c = 0.2$ in dimensionless variables corresponds to $0.2\sqrt{ED} \approx 2 \cdot 10^3$ meter per year (which seems rather fast). This confirms that the estimates

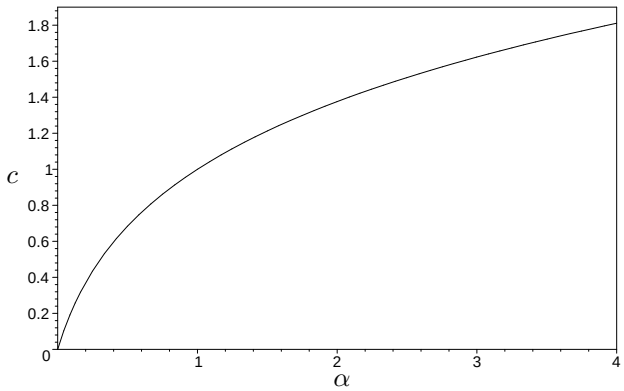

FIGURE 5. The wave speed c_h on a hard substrate as a function of α (with $\beta = 0$).

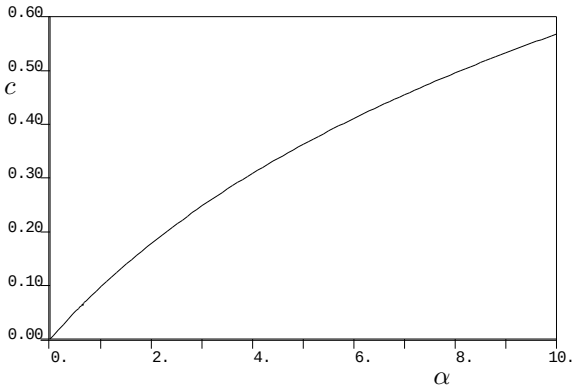

FIGURE 6. The wave speed c_s on a soft substrate as a function of α (with $\beta = 3 \cdot 10^{-2}$ and $\delta = 10^{-2}$).

of (30) may be rather inaccurate, and that α may well differ significantly from 10^{-1}.

- On the other hand, the two numbers c_h and c_s suggest that an oyster bank spreads about twenty times faster on hard substrate than on soft substrate. Despite the inaccuracy in the coefficients α, E, and D, the linear behaviour of c_h and c_s for small α (see Figs. 5 and 6) implies that the ratio

$$c_h : c_s \approx 20 : 1$$

remains valid as long as the parameters are such that the dimensionless parameter $\alpha = AFE^{-2}$ is not too large (roughly $\alpha < 1$).

While this biological conclusion is relatively easily drawn, many mathematical niceties/issues are so far unresolved, partly due to time limitations. In particular, the asymptotic regime $\beta \to 0$ for the soft substrate model has not been analysed

in depth. Besides, the limit of large α would be interesting to study from a mathematical point of view.

5. Influencing the population by reduction of salinity

The possibility of lowering the salinity of all or part of the Eastern Scheldt by once again allowing freshwater from local rivers to drain into the basin has been proposed as a method to hinder oyster population growth. It should be noted that for *raising* salinity levels (by for example turning compartments into lagoons by building more dams) to have an impact on larval production or mortality, or on oyster mortality, the salinity level would have to be taken above the tolerance of many other indigenous organisms that inhabit the bottom of the estuary, collectively called benthics.

Specifically, we have already seen (p. 27) that oyster fecundity is a function of salinity, both because oysters produce fewer larvae in less salty water and because oyster larvae have higher mortality (proportion of population succumbing to disease) in less salty water [**8**]. However, other species in the Eastern Scheldt are also sensitive to salinity levels, so for example a stratagem involving closing the storm surge barrier and flooding the Eastern Scheldt with freshwater would doubtlessly remove the vast majority of oysters, but would also presage an ecological disaster. Furthermore, since the freshwater dams were constructed between 1964 and 1987, agriculture upstream of the dams has become dependent on the current river conditions. This is in addition to the still pertinent reason for building the dams: flood prevention. With these facts in mind, a permanent reopening of the dams would not be without its side effects. In this section we will therefore consider *seasonal salinity reduction*, or *SSR*, in which freshwater would be allowed into the Eastern Scheldt only in a period coinciding with the spawning season and the life span of the larvae. In addition, and for reasons to be explained below, only SSR in the Eastern Compartment (Kom) of the Eastern Scheldt will, see figure 2, be considered. This implies that the dams in other compartments would remain intact, and the consequences for agriculture and flood prevention would be minimised.

5.1. The Eastern Compartment. The two locations for direct freshwater input are The Northern and Eastern Compartments. The Kom was chosen for analysis for several reasons. Important among these is the canal which now runs along the Eastern bank of the compartment. It splits into two canals: the Schelde-Rijn-kanaal for shipping and the Bathse Spuikanaal, both fed by the Zoommeer, a lake bordering on the Eastern Scheldt, from which it is assumed large volumes of water can be pumped due to the capacity of the lake. Agriculture is believed to be more dependent on the rivers which feed the Northern Compartment. Furthermore, the Kom is the shallowest compartment and has the most regular topography and is thus amenable to a simplified analysis.

Prior to construction of the Kom dam, RIKZ measured [**5**] the influx of freshwater into the Kom at between 50 and 70 cumecs (cubic metres per second). As a seasonal measure, freshwater flowing through sluice gates in the dam would not approach these flow rates, and so the following analysis assumes that the dam remains intact and freshwater is pumped from the canal at a rate of 100 cumecs. The

assumption is that the large body of water in the Zoommeer can provide the extra capacity, and this source can be replenished in the majority of the year when the pumps are not in operation.

5.2. Effects of lower salinity. The primary trigger for spawning is water temperature [**8**, p. 312], [**4**]: *C. gigas* are known to spawn when the temperature exceeds 20°C over a period of several weeks, although they are capable of spawning at 16°C. With large concentrations of gametes in the water, spawning tends to be highly coordinated with large colonies spawning almost in synchrony, to maximise chances of reproduction. Larvae develop in the water phase for between 15 and 30 days, during which time they are spread by water currents and diffusion.

The approximately 100 day period covering the spawning and larval phases is seen as the optimal time to reduce salinity as larvae are more susceptible to reduced salinity levels than oysters. Oysters can survive water as brackish as 10ppt (parts per thousand of chloride), while larvae will not develop in salinity levels below 11ppt. This is far below the tolerance of other benthics in the area and, even if it were possible, lowering the salinity to kill the oysters and/or larvae is therefore not an option. However, mortality, oyster respiration rates, and oyster filtration rates are affected by even a small change in conditions, through the following formulae quoted in [**8**]:

$$\text{mortality} \propto \frac{S-8}{5.5}\ , \tag{32a}$$

$$\text{respiration rate} \propto 1+\left(\frac{R_r-1}{5}\right)(20-S)\ , \tag{32b}$$

$$\text{where}\quad R_r=\begin{cases}0.0915T+1.324 & T\geqslant 20^{\circ}\text{C}\ ,\\ 0.007T+2.099 & T<20^{\circ}\text{C}\ ,\end{cases}$$

$$\text{filtration rate} \propto \frac{S-10}{10}\quad \text{for } 10<S<20\ , \tag{32c}$$

where S denotes salinity and T temperature. Note that oysters are filter feeders, actively pumping water through their feeding organs and filtering out phytoplankton, bacteria and protozoa for consumption. Filtration rate can be measured in millilitres per minute.

5.3. Pumping strategies. We introduce a time system modulo 4 (i.e. 4 corresponds to one day), with 0 at low tide, 1 at the midpoint between low and high tide, and so on, with each time phase defining a *Pumping Period* (*PP*). We assume that the tidal convection is the primary mixing mechanism for fresh and salt water in the Kom, and that mixing is highly efficient: in any PP, volumes of fresh and salt water are assumed to mix fully. Though this assumption may not hold in all circumstances, in a relatively shallow basin such as the Kom, with a tidal difference of approximately 3 metres, temperature and salinity stratification, for example, are perhaps unlikely.

As discussed above, we normalise on a pumping rate of 100 cumecs by supposing that the capacity of the canal and lake permit this rate of continual supply. Thus

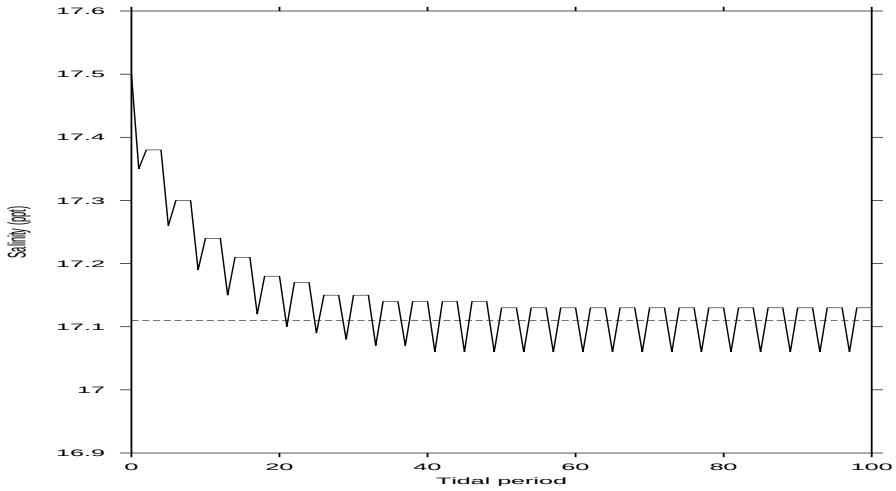

FIGURE 7. Strategy 0400

Concept	Symbol	Value
Time step	t	—
Volume at $t = n$	V_n	—
Global salinity at $t = n$	ρ_n	—
Weighting at $t = n$	W_n	Depends on strategy (mod 4)
Volume of freshwater influx in one PP	V_f	1.08
Freshwater salinity	ρ_f	0.5
Sea water salinity	ρ_s	17.5
Water volume in Kom at high tide	V	600
Water volume in Kom at low tide	v	400

TABLE 1. Table of concepts and data

a normalised freshwater input would be 1 unit per PP, and we can generate 2^4 pumping strategies within the constraint of a total of 4 units pumped during the four PPs. We shall be using the concepts, symbols and values listed in table 1, where volume is in units of 10^6m^3, and salinity is in ppt. The data were provided by RIKZ.

The formula we use to calculate the mass of salt in the Kom at time $n+1$ is the following:

$$V_{n+1}\rho_{n+1} = V_n\rho_n + W_{n+1}V_f\rho_f + (V_{n+1} - V_n - W_{n+1}V_f)M_{n+1}\ , \tag{33a}$$

$$\text{where} \quad M_{n+1} = \begin{cases} \rho_s & \text{if} \quad V_{n+1} - V_n - W_{n+1}V_f > 0. \\ \rho_n & \text{if} \quad V_{n+1} - V_n - W_{n+1}V_f < 0. \end{cases} \tag{33b}$$

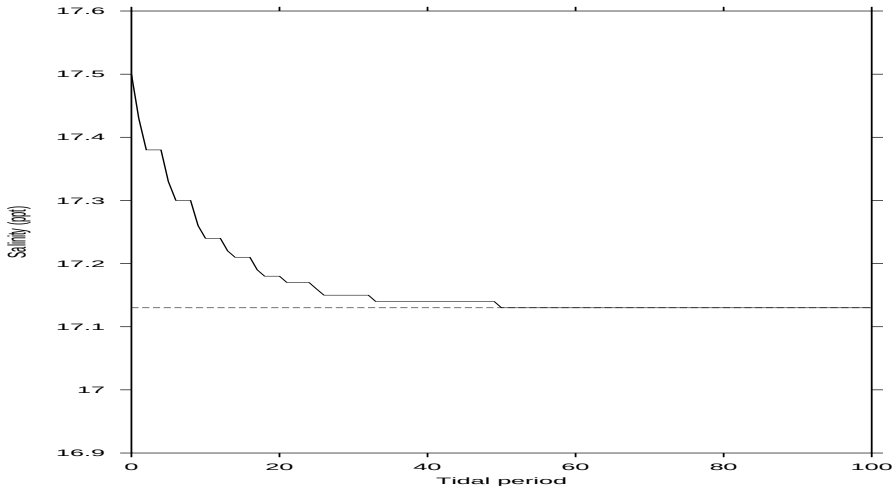

FIGURE 8. Strategy 0220

The origin of this formula is clear when it is considered term by term:

$$\begin{aligned} V_{n+1}\rho_{n+1} &\quad — \quad \text{mass of salt at } t = n+1; \\ V_n\rho_n &\quad — \quad \text{mass of salt at } t = n; \\ W_{n+1}V_f\rho_f &\quad — \quad \text{mass of salt from freshwater input;} \\ V_{n+1} - V_n - W_{n+1}V_f &\quad — \quad \text{saltwater volume change due to tidal flux.} \end{aligned} \tag{34}$$

The two cases in (33b) correspond to a rising and falling tide, respectively.

5.4. Results and Discussion. Figures 7 & 8 show SSR for two different pumping strategies. The periodic behaviour apparent here after approximately 40 time steps is a common feature of the 16 strategies considered, and suggests that pumping need only begin 5 days before spawning is predicted to start. In these two examples, the baseline (that is, mean over tidal periods) salinities after 5 days are close to each other in value. Figure 9 shows a comparison in baseline salinities for all 16 strategies, and it is clear that there is not much to choose between them in terms of baseline salinities. It is very likely that each strategy has a different engineering cost depending on the rate of pumping required, and also that some strategies may place too great a strain on water supply, and that these may become the dominant factors in deciding strategy. All strategies recover to the original baseline salinity of 18 ppt within 5 days of the freshwater supply being cut off.

It should be noted that RIKZ has conducted numerical simulations to study the effects on salinity of a *permanent* reopening of the compartment dams in both the Northern Compartment and the Eastern Compartment ([**5**]). The long-time maximum baseline salinity they predicted for the Kom is within the range covered by our SSR strategies.

We conclude by noting that SSR in the Kom has the advantages of maintaining the flood protection afforded by the compartment dams, of providing a short-term,

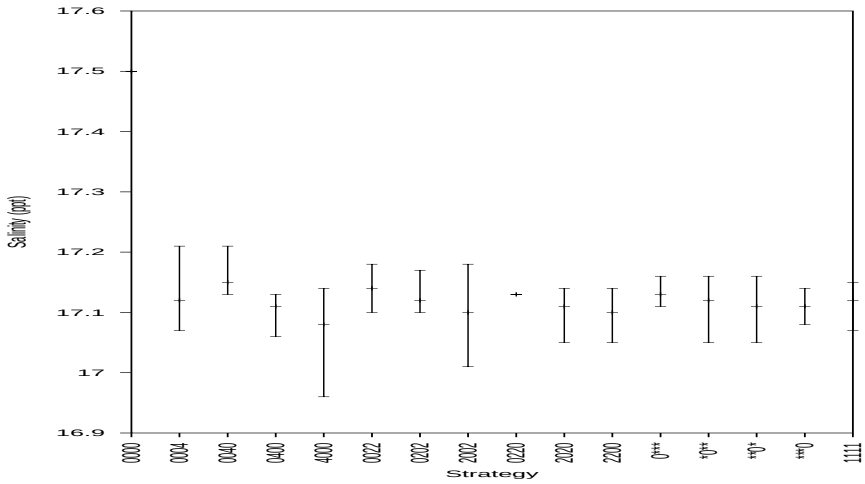

FIGURE 9. Mean salinities after 5 days of pumping are shown, along with bars representing the minimum and maximum salinities over tidal periods. For clarity, *s represent $\frac{4}{3}$.

controllable method to reduce salinity in time for the spawning and larval development periods, and of allowing farmed oyster production — with beds created by "planting" imported young oysters — to continue in the Kom. There may even be additional benefits associated with importing water from Lake Zoommeer. These could include a decrease in water temperature in the Kom, and an increase in suspended sediment — both of which have negative impacts on spawning and survival rates, see for example [**8**]. However, the scheme has the disadvantage of only lowering salinity by $2 - -3\%$ in the Kom which, through the formulae (32), could lead to an increase in larval mortality of approximately 4%. There is also an associated decrease in oyster filtration rate of around 5%, and an *increase* in oyster respiration of around 10% for a summer water temperature of 22°C.

Consuming less food and utilising more stored energy supplies will presumably impact on the number of gametes each oyster is capable of producing, and a quantitative link would be of use. Less food removed from the water column also implies more is available for other species.

The above analysis rests on many simplifications of the system, and any final recommendation on the viability of SSR would have to rest on a more complete numerical model similar to that used by RIKZ in their long-time simulations. However, we believe that the data obtained gives reasonable estimates for the likely effects of SSR in the Kom, and is seems clear that the salinity cannot be reduced sufficiently to make this approach feasible.

6. Outline of a large-scale simulation

For a more detailed answer to the questions of the Introduction we propose the use of large-scale computer simulation to reconstruct and to predict the development of the oysters.

6.1. How are the oyster clusters formed? In the following we give a sketch of the life cycle of a Japanese oyster. Most data are taken from the report [**7**].

1 eggs (in July-August an adult oyster produces between 10^6 and 10^8 eggs);
2 larvae (an egg together with sperm develop into a larvae within 1 day);
3 veliger larvae (in one or two days the larvae develop into veliger larvae (with larval shell));
4 spat (in 15 to 30 days they settle down on appropriate hard substrate, bigger larvae can crawl quite a distance searching for approriate settlement);
5 juvenile oysters develop into adult oysters after one year (estimated mortality of juvenile eastern oysters of more than 64% in seven days after settlement and more than 86% in one month after settlement on sub-tidal and inter-tidal plates);
6 death (caused by aging (it has been estimated a Japanese oyster can live approximately 20 years); the other major causes of death for oysters in general, such as predators and diseases, are not substantial in the Eastern Scheldt).

A simplified view of how a new cluster/colony arises is the following:

The larvae floating in water are displace by diffusion and carried with the tidal movement. Within 3 weeks they have to settle down on appropriate substrates (hard surface) or otherwise die. The settling down occurs at the moment when the water is quiet (e.g., at the turn of a tide, approximately 20 minutes, or in quiet surroundings). After settling down they will stay there, however, a large percentage of them die before reaching adulthood. After one year, those surviving (juvenile) oysters will enter the reproduction system and start to produce gametes and eggs. Oyster clusters are formed or grow when (veliger) larvae settle down on appropriate substrates and survive there.

6.2. Diffusion and convection of larvae due to tides. Two main factors, determining the place for the larvae to settle down, are: 1) advection and diffusion of the tidal flow; and 2) to be at the appropriate place while the water is quiet. If we ignore the swimming effect of the larvae, the transport of larvae can be described by the shallow water equations,

$$\frac{\partial u}{\partial t} = -u\frac{\partial u}{\partial x} - v\frac{\partial u}{\partial y} - w\frac{\partial u}{\partial z} + fv - g\frac{\partial \zeta}{\partial x} + \nu_h\frac{\partial^2 u}{\partial x^2} + \nu_h\frac{\partial^2 u}{\partial y^2} + \frac{\partial}{\partial z}\left(\nu_v\frac{\partial u}{\partial z}\right) \tag{35}$$

$$\frac{\partial v}{\partial t} = -u\frac{\partial v}{\partial x} - v\frac{\partial v}{\partial y} - w\frac{\partial v}{\partial z} - fu - g\frac{\partial \zeta}{\partial y} + \nu_h\frac{\partial^2 v}{\partial x^2} + \nu_h\frac{\partial^2 v}{\partial y^2} + \frac{\partial}{\partial z}\left(\nu_v\frac{\partial v}{\partial z}\right) \tag{36}$$

$$w = -\frac{\partial}{\partial x}\left(\int_{-d}^{z} u\,dz'\right) - \frac{\partial}{\partial y}\left(\int_{-d}^{z} v\,dz'\right) \tag{37}$$

$$\frac{\partial \zeta}{\partial t} = -\frac{\partial}{\partial x}\left(\int_{-d}^{\zeta} u dz\right) - \frac{\partial}{\partial y}\left(\int_{-d}^{\zeta} v dz\right) \tag{38}$$

and the transport equation with c being the concentration of larvae:

$$\frac{\partial c}{\partial t} = -\frac{\partial uc}{\partial x} - \frac{\partial vc}{\partial y} - \frac{\partial wc}{\partial z} + \frac{\partial}{\partial x}\left(D_h \frac{\partial c}{\partial x}\right) + \frac{\partial}{\partial y}\left(\frac{\partial c}{\partial y}\right) + \frac{\partial}{\partial z}\left(D_v \frac{\partial c}{\partial z}\right) \tag{39}$$

Here the triplet (u, v, w) is the velocity vector, f the Coriolis parameter, g the gravitational acceleration, and ν_h/ν_v and D_h/D_v the horizontal and vertical viscosities and diffusion (or dispersion) coefficients. The function ζ is the height of the water surface.

The shallow water equations governing the water movement can be simulated using the existing simulation model TRIWAQ (which is in operational use at Rijkswaterstaat [**18, 16**]), and the transport equation can be simulated with a particle simulation model SIMPAR (a 2-dimensional version is also in operational use at Rijkswaterstaat [**2, 6**], and a 3-dimensional model is currently being developed at TU Delft [**13, 14**]) using the flow velocity data produced by TRIWAQ. Instead of looking at the concentration of larvae, we consider the discrete (likely aggregated into groups of larvae) quantity which are 'particles' carried with the water movement. For that the continuous transport equation (in concentration) is transformed into a stochastic partial differential equation (e.g., Fokker-Planck equation).

With the above simulation models we can determine the position of the larvae at the time when the water is quiet. If a larva happens to be positioned above an appropriate (preferably hard) surface, then there is a certain chance that it will settle down on that surface. There exist quite detailed geometry and geological data about the Eastern Scheldt which can be used for the simulation. The geometry data (e.g. depth) are already used by TRIWAQ and SIMPAR, but we need additional geological data (hard, soft surfaces) for our simulation of the distribution of the oysters. The main problem remaining here is to simulate the life cycle of the oysters in order to determine the speed of population increase, reconstruction of the past development and prediction of future development, etc.

6.3. Simulation of the life cycle of oysters. In section 6.1 we have described the life cycle of an oyster. In order to obtain detailed information of the spread of the oysters we need to model the important factors which affect the development of oysters.

We may distinguish this life cycle into two major phases:

Phase 1. Each year in July there is a moment when oysters (older than 1 year) start to produce eggs and gametes. Then there will be billions of eggs and gametes or larvae floating in the water (initially above the spawning oyster colonies). This can be modelled as (multiple) sources in the transport model SIMPAR. The number of larvae produced by a single oyster depends on many factors: size of the oyster, environmental conditions, etc. (see the discussion in Section 3).

Phase 2. This is the period from the moment of settling down to developing into an adult oyster. During this period the oyster will stay in the same place except when they are very young (spat, juvenile oyster). In the latter case they can be

wiped out by strong currents. From juvenile oyster to adult oyster, we know that a large percentage will die before reaching adulthood.

In general, there are five biotic factors causing oyster death: disease, predation, competition, developmental complications, and energy depletion. And there are five abiotic factors: moisture depletion, temperature, salinity, water motion, and oxygen depletion. Disease and predation are said to have the greatest effect on oyster populations. However, as mentioned earlier, these two factors are not significantly present in the Eastern Scheldt. Which factors contribute predominantly to the death or survival of the Japanese oysters in this specific Eastern Scheldt remains to be investigated.

To conclude: many factors for the model of the life cycle of a Japanese oyster still need to be investigated, part of them can be determined by experiments, and part of them can be determined/tuned by comparing simulation results with the past observational data.

A. Appendix: derivation of (14)

Consider equation (3) where u is given by (11). Let us rescale the space and time variables as

$$\begin{pmatrix} X & Z & T \end{pmatrix} = \begin{pmatrix} x/L & z/h & U_0 t/L \end{pmatrix}, \tag{40}$$

where L is a characteristic scale in the x-direction. From the shallowness hypothesis, we assume that $h = \epsilon L$, $\epsilon \ll 1$. Then, introducing the Peclet number $P_e = \frac{U_0 h}{D}$, equation (3) becomes

$$\epsilon P_e \left(\frac{\partial \mathcal{L}}{\partial T} + v\left(Z\right) \frac{\partial \mathcal{L}}{\partial X} \right) = \frac{\partial^2 \mathcal{L}}{\partial Z^2}, \tag{41}$$

$$v\left(Z\right) = \frac{3}{2} \frac{\left(Z - Z_0\right)\left(2 - Z - Z_0\right)}{\left(1 - Z_0\right)^2}, \tag{42}$$

with no-flux boundary conditions at $Z = 0, 1$:

$$\frac{\partial \mathcal{L}}{\partial Z} = 0, \quad Z = 0, 1. \tag{43}$$

The presence of the small number $\epsilon P_e \ll 1$, suggests to seek a solution in series of power of ϵP_e in the form

$$\mathcal{L} = \mathcal{L}_0\left(X, Z, T; \tau\right) + \epsilon P_e \mathcal{L}_1\left(X, Z, T; \tau\right) + \ldots, \tag{44}$$

where τ is a slow timescale defined by $\epsilon P_e T$. Inserting (44) into (41), we find at leading order that

$$\mathcal{L}_0\left(X, Z, T; \tau\right) = \mathcal{L}_0\left(\xi; \tau\right), \quad \xi = X - T, \tag{45}$$

while the solution at order $\left(\epsilon P_e\right)^2$ is

$$\mathcal{L}_1\left(X, Z, T; \tau\right) = -\frac{\left[\left(-2 + Z\right) Z + 2 Z_0\left(X\right) - Z_0^2\left(X\right)\right]^2}{8\left[-1 + Z_0\left(X\right)\right]^2} \frac{\partial \mathcal{L}_0}{\partial \xi}. \tag{46}$$

Finally at order $(\epsilon P_e)^2$, equation (41) reads

$$\frac{\partial^2 \mathcal{L}_2}{\partial Z^2} = F\left(\frac{\partial \mathcal{L}_0}{\partial \tau}, \frac{\partial \mathcal{L}_0}{\partial \xi}, \frac{\partial^2 \mathcal{L}_0}{\partial \xi^2}, Z, Z_0\right). \tag{47}$$

The form of F is rather complicated and of no real interest so we do not explicitate it here. The key point is that $\mathcal{L}_2$ has to satisfy the boundary conditions (43) and this yields the solvability condition

$$\int_0^1 F\left(\frac{\partial \mathcal{L}_0}{\partial \tau}, \frac{\partial \mathcal{L}_0}{\partial \xi}, \frac{\partial^2 \mathcal{L}_0}{\partial \xi^2}, Z, Z_0\right) dZ = 0.$$

After integration, we obtain

$$\frac{\partial \mathcal{L}_0}{\partial \tau} = -\frac{24\,(1-Z_0)}{105}\frac{dZ_0}{dX}\frac{\partial \mathcal{L}_0}{\partial \xi} + \left(\frac{1}{P_e^2} + \frac{2\,(1-Z_0)^2}{105}\right)\frac{\partial^2 \mathcal{L}_0}{\partial \xi^2}, \tag{48}$$

which, in terms of the original space and time variables x and t, is (5).

Bibliography

[1] J. R. Dew, A population dynamic model assessing options for managing eastern oysters (*Crassostrea virginica*) and triploid Suminoe oysters (*Crassostrea ariakensis*) in Chesapeake Bay, MS Thesis. Virginia Polytechnic Institute and State University, 2002.

[2] M. Elorche, Vooronderzoek Particle-module in SIMONA (in Dutch). *Werkdocument RIKZ/OS-94.143x*, 1994.

[3] A. Gangnery, C. Bacher, and D. Buestel, *Assessing the production and the impact of cultivated oysters in the Thau lagoon (Mediterranee, France) with a population dynamics model*, Can. J. Fish. Aquat. Sci. **58**, pp. 1012–1020, 2001.

[4] P. Goulletquer *et al*, *La reproduction naturelle et controlée des Bivalves cultivés en France*, IFREMER Rapport Interne DRV/RA/RST/97-11 RA /Brest, 1997.

[5] H. Haas and T. Tosserams, *Balanceren tussen zoet en zout* en *Ruimte voor veerkracht en veiligheid in de Delta*, Rapporten RIKZ/2001.18 en RIZA/2001.014.

[6] A. W. Heemink, Stochastic Modeling of dispersion in shallow water. *Stochastic Hydrol. Hydraul.* 4, pp. 161–174, 1971.

[7] B.J. Kater, Japanse oesters in de Oosterschelde: ecologisch profiel, RIVO Report (in Dutch), April 2003.

[8] M. Kobayashi, *et al*, *Aquaculture* **149**, pp. 285–321, 1997.

[9] R. Mann, & D. A. Evans, Estimation of oyster, *Crassostrea virginica*, standing stock, larval production, and advective loss in relation to observed recruitment in the James River, Virginia, *J. Shellfish res.*, 17(1), pp. 239-253, 1998.

[10] J. D. Murray, *Mathematical biology; an introduction.*

[11] J. R. Ockendon, S. D. Howison, A. A. Lacey, and A. B. Movchan, *Applied Partial Differential Equations*, Oxford University Press 1999

[12] D. B. Quayle, Pacific oyster culture in British Columbia, *Fish. Res. Board. Can. Bull.*, 169, pp 1–192, 1969.

[13] J. W. Stijnen & H. X. Lin, The Modeling of Diffusion in Particle Models, Project Report to National Institute for Coastal and Marine Management (RIKZ), Contract RIKZ/OS 2000/06080, 14 p., September 2000.

[14] J. W. Stijnen, A. W. Heemink & H. X. Lin, An Efficient 3D Particle Transport Model for Use in Stratified Flow *to be published.*.

[15] G. I. Taylor, *Dispersion of soluble matter in a solvent flowing slowly through a tube*, Proc. Roy. Soc. **A210**, pp. 186-203.

[16] E. A. H. Vollebregt, Parallel Software Developemnt Techniques for Shallow Water Models, Ph.D. Thesis, Delft Unversity of Technology, 1997.

[17] T. Yanagi, *A simple method for estimating ...*, see `http://data.ecology.su.se/MNODE/Methods/YanagiMixing/Yanagi.htm`.

[18] M. Zijlema, TRIWAQ - three-dimensional incompressible shallow flow model, *Technical Documentation*, RIKZ/Rijkwaterstaat, 1997.